MBE Advance Access published April 12, 2016

Optimization of Conformational Dynamics in an Epistatic Evolutionary Trajectory

Mariano M. González[1], Luciano A. Abriata[†,1], Pablo E. Tomatis[1] and Alejandro J. Vila[*,1,2]

[1]IBR (Instituto de Biología Molecular y Celular de Rosario), Consejo Nacional de Investigaciones Científicas y Técnicas (CONICET), Facultad de Ciencias Bioquímicas y Farmacéuticas, Universidad Nacional de Rosario, Ocampo y Esmeralda, Rosario, Argentina

[2]Plataforma Argentina de Biología Estructural y Metabolómica (PLABEM), Ocampo y Esmeralda, Rosario, Argentina

[†]Present address: Laboratory for Biomolecular Modeling and Swiss Institute of Bioinformatics, Swiss Federal Institute of Technology, EPFL, Lausanne, Switzerland

*Corresponding author: E-mail: vila@ibr-conicet.gov.ar.

Associate editor: Miriam Barlow

Abstract

The understanding of protein evolution depends on the ability to relate the impact of mutations on molecular traits to organismal fitness. Biological activity and robustness have been regarded as important features in shaping protein evolutionary landscapes. Conformational dynamics, which is essential for protein function, has received little attention in the context of evolutionary analyses. Here we employ NMR spectroscopy, the chief experimental tool to describe protein dynamics at atomic level in solution at room temperature, to study the intrinsic dynamic features of a metallo-β-lactamase enzyme and three variants identified during a directed evolution experiment that led to an expanded substrate profile. We show that conformational dynamics in the catalytically relevant microsecond to millisecond timescale is optimized along the favored evolutionary trajectory. In addition, we observe that the effects of mutations on dynamics are epistatic. Mutation Gly262Ser introduces slow dynamics on several residues that surround the active site when introduced in the wild-type enzyme. Mutation Asn70Ser removes the slow dynamics observed for few residues of the wild-type enzyme, but increases the number of residues that undergo slow dynamics when introduced in the Gly262Ser mutant. These effects on dynamics correlate with the epistatic interaction between these two mutations on the bacterial phenotype. These findings indicate that conformational dynamics is an evolvable trait, and that proteins endowed with more dynamic active sites also display a larger potential for promoting evolution.

Key words: **protein evolution, epistasis, conformational dynamics.**

Introduction

One important challenge in the field of protein evolution is to dissect the contributions of biochemical and biophysical traits to protein function and, ultimately, to organismal fitness (DePristo et al. 2005). This endeavor is largely complicated by the fact that, in many cases, the impact of mutations on fitness follows sign epistasis (Beadle and Shoichet 2002; DePristo et al. 2005; Weinreich et al. 2006; Tokuriki et al. 2008; Salverda et al. 2011; Breen et al. 2012; Pollock et al. 2012; Gong et al. 2013; Natarajan et al. 2013; Gong and Bloom 2014; Mehta et al. 2015; Meini et al. 2015), such that the effects of mutations depend on the genetic background where they take place. However, the understanding of how epistatic couplings operate at the atomistic level to affect protein traits is insufficient, mostly due to the pleiotropic effect of mutations.

Fitness can often be quantitatively described based on the biochemical and biophysical traits affected by mutations along protein evolution pathways (DePristo et al. 2005; Liberles et al. 2012; Abriata et al. 2015). Protein function and stability are undoubtedly the key features affected by mutations. However, both function and stability are intimately linked to protein conformational dynamics, which is essential for any biological process (Tokuriki and Tawfik 2009; Tokuriki et al. 2009; Palmer 2015; Kay 2016). Protein dynamics is well known to play key roles in protein–protein recognition, ligand binding, allostery, and catalysis, therefore representing a potentially important constraint to protein evolution as recently discussed (Boehr et al. 2009; Jackson et al. 2009; Afriat-Jurnou et al. 2012; Liu and Bahar 2012; Kaltenbach and Tokuriki 2014; Dellus-Gur et al. 2015; Zou et al. 2015). This idea has been put forward based on the variability observed in crystallographic structures of different variants of a protein, or of same proteins bound to different ligands, and through molecular dynamics simulations, but these approaches suffer from important limitations. On one hand, atomistic simulations are still far from reaching the multimicrosecond and millisecond timescales on which catalytically relevant protein dynamics take place, even for unbiased enhanced-sampling methods (Lindahl 2015; Perez et al. 2016). Coarse-grained methods barely reach these timescales, but anyway they are not designed to study fine conformational dynamics; while normal mode-based methods only give a very coarse representation of dynamics without the atomic or residue level of detail required for fine investigations. On the other hand, X-ray structures report snapshots of the ground conformational

Article

protein state trapped during crystal packing. Although informative, the crystallization conditions or even ligand binding can induce apparent dynamics that may not exist in the intrinsic conformational landscape of the free protein.

A powerful alternative stands in Nuclear Magnetic Resonance (NMR), a spectroscopic technique that allows monitoring protein dynamics at the atomistic level in solution and at room temperature (Lisi and Loria 2016). Enzyme-catalyzed reactions and binding events usually occur on the microsecond (μs) to millisecond (ms) timescale (Villali and Kern 2010; Palmer 2015). Therefore, protein dynamics within this range is expected to be favored in evolution when required. The available suite of NMR experiments can probe a wide range of motional regimes ranging from picosecond (ps) to seconds (s) (Palmer 2015).

In previous works, we have used β-lactam resistance mediated by *Bacillus cereus* metallo-β-lactamase (MBL) II (BcII hereafter) as a model system for dissecting the mechanisms of protein evolution. Here we utilize NMR for the characterization of four BcII variants identified by directed molecular evolution studies. Experimental studies of the evolutionary trajectory started from wild-type BcII (Tomatis et al. 2005; Meini et al. 2015) revealed enzymatic activity and Zn(II) affinity as the dominant traits in this model system. These studies also showed that changes in protein stability cannot explain the effects observed on fitness, in contrast to other systems (Beadle and Shoichet 2002; Wang et al. 2002; DePristo et al. 2005; Weinreich et al. 2006). In the favored evolutionary trajectory, two mutations (Gly262Ser and Asn70Ser) displaying strong sign epistasis on catalysis and resistance increased the activity against cephalexin by two orders of magnitude with respect to the wt enzyme (Tomatis et al. 2008). Mutation Gly262Ser is responsible for a large increment in the activity toward cephalexin but is detrimental for the Zn(II) binding affinity. Mutation Asn70Ser, in contrast, is deleterious for wt BcII performance. However, when present in the Gly262Ser background, Asn70Ser is a compensatory mutation that restores Zn(II) affinity, giving rise to a higher resistance phenotype (Meini et al. 2015).

The accumulation of these two mutations also resulted in an increased activity against at least four other β-lactam substrates of different subclasses (cefotaxime, ceftazidime, penicillin G, and imipenem) implying that the enzyme substrate spectrum is not sacrificed, but instead, enhanced. The improved activity on these substrates cannot be explained based on the crystal structure of the evolved enzyme (Tomatis et al. 2008). In general, expansion of the substrate profile in enzymes is attributed to conformational dynamics (Maurice et al. 2008; Tokuriki and Tawfik 2009; Zou et al. 2015), while quenching the native dynamics can be deleterious for the enzyme activity (Bhabha et al. 2011).

In this work, using NMR relaxation experiments we have specifically addressed the role of protein dynamics in two evolutionary pathways of the MBL BcII toward a double mutant with expanded substrate profile. We report that 1) NMR identifies precise perturbations in the protein structure and dynamics that account for the effect of mutations in the affinity for Zn(II); 2) the impact of the mutations on dynamics strongly depends on the genetic context, that is, is epistatic; and 3) the successful pathway accumulates mutations successively increasing loop dynamics, chiefly in the micro- to millisecond timescales. Overall, these results allow us to conclude that conformational dynamics over a timescale relevant for substrate binding and catalysis is an evolvable trait that can be optimized, in order to provide the fine tuning that the active site requires to accommodate new substrates.

Results

We initiated our work performing a detailed characterization of the four BcII variants using NMR. The BBL (B Beta-Lactamases) numbering scheme for class B β-lactamases was used throughout this work (Garau et al. 2004). Samples of wild-type (wt BcII), Asn70Ser, Gly262Ser, and Gly262Ser/Asn70Ser versions of BcII were expressed and purified by using appropriate labeling strategies, as detailed in the Methods section. Samples were stable enough for their analysis by NMR and were prepared in 100 mM 2-(N-morpholino)ethanesulfonic acid (MES) pH 6.4 with 200 mM NaCl and 10% D_2O. Supplementary figure S1, Supplementary Material online, shows the ^{1}H-^{15}N HSQC spectra of the four MBLs variants. HSQC NMR spectra are basically fingerprints made up of cross-peaks between pairs of N and H resonances corresponding to the N–H groups of the protein backbone. All spectra display good signal dispersion indicating that all enzymes are properly folded, allowing us to discard the presence of unfolded or misfolded forms.

Resonance Assignment of MBLs

The first step in any NMR investigation is to assign each of the cross-peaks in an HSQC spectrum to the corresponding residue in the protein. The complete backbone and side-chain resonance assignments of wt BcII available in the literature were adapted to our experimental conditions (Karsisiotis et al. 2014). Backbone resonances for BcII Asn70Ser, BcII Gly262Ser, and BcII Gly262Ser/Asn70Ser were assigned on the basis of the three-dimensional HNCO, HN(CA)CO, HN(CO)CA, HNCA, CBCA(CO)NH, and HNCACB spectra performed on ^{15}N, ^{13}C-doubly labeled samples (Gardner and Kay 1998).

Of the 222 nonproline residues (proline lacks a backbone H and hence N–H correlations) in the amino acid sequences of the four variants, we unambiguously assigned 211 backbone amide resonances for wt BcII, 211 for BcII Asn70Ser, 206 for BcII Gly262Ser, and 205 for BcII Gly262Ser/Asn70Ser. In wt BcII and in the Asn70Ser mutant, the 11 nonproline residues that could not be assigned in the ^{1}H-^{15}N HSQC spectra are the following: The three N-terminal residues (Ser27, Gln28, Lys29), Lys50, Asn62, Ser77, Lys102, Ala119, Asn184, Gly193, and Asn233. Assignments for these residues were also missing in the Gly262Ser and Asn70Ser/Gly262Ser variants, together with residues Ile96, Cys221, Lys224, Gly264, and Leu283 in Gly262Ser and Asp120, Cys221, Val223, Lys224, Gly264, and Leu283 in Gly262Ser/Asn70Ser, most of which are located near the active site. Overall, we have been successful in assigning more than 90% of the detectable residues in each variant, which permit us to carry out a detailed characterization using NMR.

Selective Effects on the Zn Sites

The active site of BcII hosts two Zn(II) ions in a shallow groove flanked by loops L3 and L10. The Zn1 site is coordinated to His116, His118, and His196, and a hydroxide ion; and the Zn2 site is bound to Asp120, Cys221, and His263, a water molecule, and to the former hydroxide which bridges both metal ions (fig. 1*A*). These metal-binding residues (metal ligands) in the active site are located in protein loops (L7, L9, L10, and L12) which define the active site floor. A hydrogen bond network spans the base of the active site, involving residues Asn70, Arg121, and Gly262 (from loops L3, L7, and L12, respectively).

The positions of the resonances in the HSQC spectra pinpoint the chemical shifts of the ^{1}H and ^{15}N nuclei for each amide bond in the studied protein, which are in turn very sensitive to the immediate environment of these nuclei. This allows us to follow the impact of mutations in remote sites of the protein at the residue level.

Mutations Gly262Ser and Asn70Ser elicited distinct chemical shift perturbation (CSP) profiles on the NMR spectra (supplementary figs. S2 and S3 and tables S1 and S5, Supplementary Material online), mostly affecting the Zn ligands, as well as other residues located in some of these loops. In addition, some resonances became broadened beyond the detection limit in mutants Gly262Ser BcII (Ile96, Cys221, Lys224, Gly264, and Leu283) and Gly262Ser/Asn70Ser BcII (Asp120, Cys221, Val223, Lys224, Gly264, and Leu283) with respect to wt BcII. This broadening phenomenon suggests the presence of exchange processes (i.e., dynamics) in the ms-to-seconds timescale regime induced by these mutations (Palmer 2015). In contrast, no further resonances were broadened in mutant Asn70Ser BcII.

Mutation Gly262Ser induces significant shifts in resonances from His116, His118 (Zn1 ligands), Asp120, His263 (Zn2 ligands), Asn70, and Arg121. His196 is almost unaffected in all variants. Cys221 was exchange-broadened in the HSQC spectrum of Gly262Ser BcII, preventing analysis of changes in the chemical shifts, but disclosing a perturbation in the dynamic features of this residue. On the other hand, mutation Asn70Ser exerts a smaller perturbation than mutation Gly262Ser (His263 remains almost unaffected).

Mutation Asn70Ser, when introduced into the single mutant Gly262Ser BcII, elicits specific CSPs on resonances from residues in the Zn2 environment (His263, Arg121, and Ser262) and exchange broadening in the Zn2 ligand Asp120, while Zn1 ligands and second-shell residues are largely unaffected. Thus, mutation Gly262Ser perturbs both metal binding sites, while mutation Asn70Ser mostly affects the Zn2 site. This phenomenon is more pronounced and focused in the Zn2 site when operative in the Gly262Ser genetic background relative to the wild-type background. NMR thus pinpoints the selective compensatory effect of mutation Asn70Ser on the binding affinity of the Zn2 site.

This analysis allowed us to identify precise and selective perturbations exerted by each mutation along the evolutionary pathway of BcII. In addition, the exchange broadening of resonances beyond the detection limit is indicative of conformational dynamics around a ms timescale.

Slow Protein Dynamics Is Enhanced along the Favored Evolutionary Pathway

The previous NMR analyses of the BcII variants suggested the presence of dynamics, mainly in the evolved variants BcII Gly262Ser and BcII Gly262Ser/Asn70Ser. Therefore, we carried out NMR relaxation experiments specifically tailored to probe the conformational dynamics in a wide timescale from ps to seconds, in the four variants.

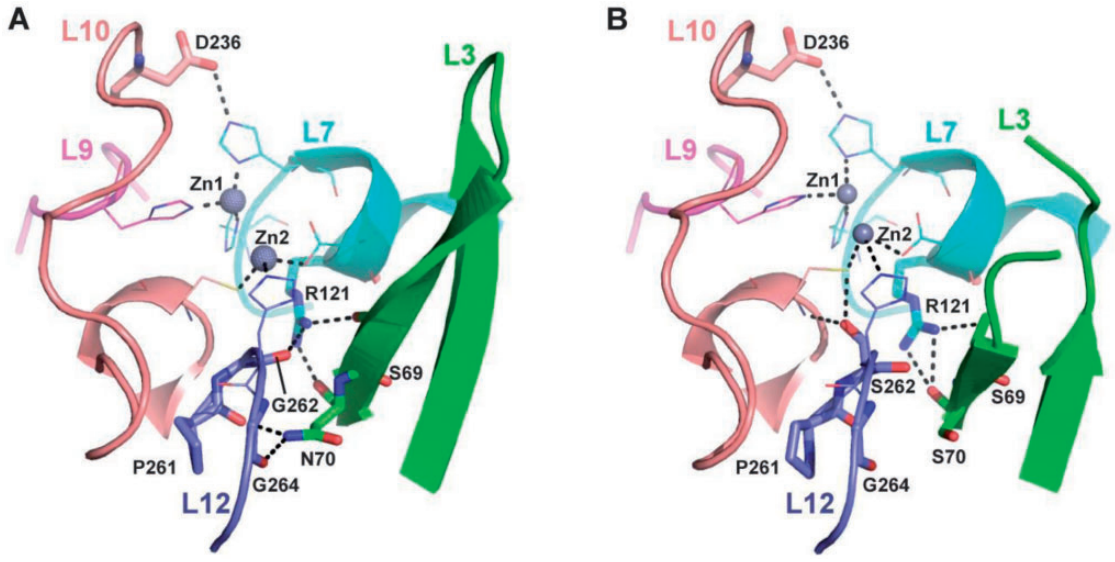

Fig. 1. Upper views of the active sites of (*A*) wild-type BcII (PDB ID 4NQ4) and (*B*) evolved BcII containing mutations Gly262Ser and Asn70Ser, as well as mutations Val112Ala and Leu250Ser (PDB ID 3FCZ) (Tomatis et al. 2008). The loops flanking the active site (L3 and L10) and those containing the metal ligands (L7, L9, and L12) are depicted, together with relevant active site residues. Zn(II) ions are shown as spheres. Metal ligands are shown as lines, residues at positions 69, 70, 121, 236, 261, and 262 are shown as sticks, and hydrogen bonds are indicated by black dashed lines.

Pico- to Nanosecond Timescale Dynamics

We characterized the effects of mutations on the picosecond-to-nanosecond (ps–ns) timescale dynamics, by measuring the R_1 and R_2 relaxation rates and ^{1}H-^{15}N Nuclear Overhauser Effects (NOEs) for backbone amide ^{15}N nuclei. These values together with the order parameter S^2 calculated from these experimental data are plotted as a function of residue number in supplementary figure S4, Supplementary Material online, for all variants. The order parameter S^2 ranges from 0 (isotropic disordered motion) to 1 (rigid) (Lipari and Szabo 1982a, 1982b; Jarymowycz and Stone 2006). The four BcII variants are highly ordered in the ps–ns timescale, exhibiting a relatively rigid backbone along the entire protein sequence with an average $S^2 = 0.9 \pm 0.1$ (supplementary fig. S4, Supplementary Material online). The order parameters for residues from the active site loops are similar for all variants, although some residues show S^2 values smaller than average, especially in Gly262Ser/Asn70Ser BcII.

Micro- to Millisecond Timescale Dynamics

Slow-timescale motions were examined by Car-Purcell-Meiboom-Gill (CPMG)-based ^{15}N R_2 relaxation dispersion experiments, which are targeted to probe chemical exchange phenomena that involve alternative protein conformations in the µs–ms timescale (Loria et al. 1999; Boehr et al. 2006; Kay 2016). Residue-specific relaxation dispersion profiles (ΔR_2 values) at a magnetic field strength of 600 MHz and 298 K were recorded for all four variants. Figure 2 shows plots of ΔR_2 versus residue number for each enzyme, in which ΔR_2 is the difference between R_2 values measured at CPMG frequencies of 33 and 966 Hz, which corresponds to the exchange contribution to relaxation. We stress here that our results and conclusions do not depend on fits or assumptions about the conformations of alternative conformational states nor their populations as analyzed in other more complex works (Korzhnev and Kay 2008). The residues in conformational exchange are mapped onto the structure of each variant in figure 3A. In wild-type BcII, only five residues were characterized by significantly high ΔR_2 values (using NESSY software as detailed in Methods) and therefore found to undergo significant conformational exchange: Leu48, Arg107, Gly132, Ile133, and Cys221. All these residues, with the exception of Cys221 (one of the zinc ligands of the Zn2 site located in loop L10), are far away from the active site in solvent-exposed regions of the protein (figs. 2C and 3A).

Mutant Asn70Ser did not show significant exchange broadening, suggesting that the few µs–ms dynamic features observed in wt BcII are quenched by mutation Asn70Ser (figs. 2D and 3A).

In contrast, mutants Gly262Ser and Gly262Ser/Asn70Ser exhibited conformational dynamics in several residues located near the active site (fig. 3). This is the case for 19 residues in Gly262Ser BcII which map mainly to the active site loops L7 and L10 (figs. 2B and 3A). This conformational dynamics (supplementary figs. S5–S7 and tables S2–S4, Supplementary Material online) is expanded in the double mutant Gly262Ser/Asn70Ser BcII in which 28 residues mapping to loops L3, L7, L10, and L12 become flexible (fig. 2A and 3A). The fact that this dynamics is not observed in the single mutant Asn70Ser reveals that this mutation only can elicit dynamics in the Gly262Ser genetic background.

Millisecond to Second Timescale Dynamics

As pointed out when the resonance assignment was described, signals from 11 residues are missing in the ^{1}H,^{15}N-HSQC spectrum of the four variants: The three N-terminal residues (Ser27, Gln28, Lys29), Lys50, Asn62, Ser77, Lys102, Ala119, Asn184, Gly193, and Asn233. This observation suggests that these resonances can be under exchange in the millisecond-to-seconds timescale.

Interestingly, some residues near the active site are broadened only in the evolved mutants: Cys221 presents µs–ms timescale conformational exchange in the wild-type enzyme (supplementary table S2, Supplementary Material online); however, its NH cross-peak is not detected in the ^{1}H^{15}N-HSQC spectrum of Gly262Ser and Gly262Ser/Asn70Ser mutants implying that mutation Gly262Ser alters a conformational process of Cys221 from nearly slow to intermediate rate in the chemical shift timescale in both variants (supplementary table S5, Supplementary Material online). A similar effect is observed for residues Asp120 and Val223: These residues present conformational exchange in BcII Gly262Ser (supplementary table S3, Supplementary Material online) but are broadened beyond detection in Gly262Ser/Asn70Ser (supplementary table S5, Supplementary Material online). On the other hand, Gly264 has no conformational exchange in wild-type and Asn70Ser variants but is broadened in both Gly262Ser and Gly262Ser/Asn70Ser (supplementary table S5, Supplementary Material online), whereas Lys224, detected in the ^{1}H^{15}N-HSQC as an overlapped signal in both wild-type and Asn70Ser, is not detected in Gly262Ser and Gly262Ser/Asn70Ser mutants (supplementary table S5, Supplementary Material online). Thus, slow dynamics around the ms timescale is observed in residues near the active site in Gly262Ser and Gly262Ser/Asn70Ser BcII.

Discussion

Recent studies have provided evidence about the importance of remote mutations in protein evolution by fine-tuning active site features (Oelschlaeger et al. 2005; Natarajan et al. 2013; Risso et al. 2015; Zou et al. 2015). Trapping of different conformations in crystal structures has suggested that the main role of these mutations is their effect on protein stability and/or protein dynamics. However, these structural snapshots could well represent induced-fit states without implying true perturbations of the intrinsic protein dynamics present in the substrate-free protein. Molecular dynamics simulations have been used to test the effect of mutations on an enzyme's conformational landscape, but unfortunately these computational methods fall short in accurately describing long-timescale dynamics compatible with substrate binding and catalysis (Lindahl 2015; Perez et al. 2016). In this study, we used NMR spectroscopy to quantitate the intrinsic protein conformational dynamics along two short evolutionary pathways resulting from an in vitro evolution experiment. To this

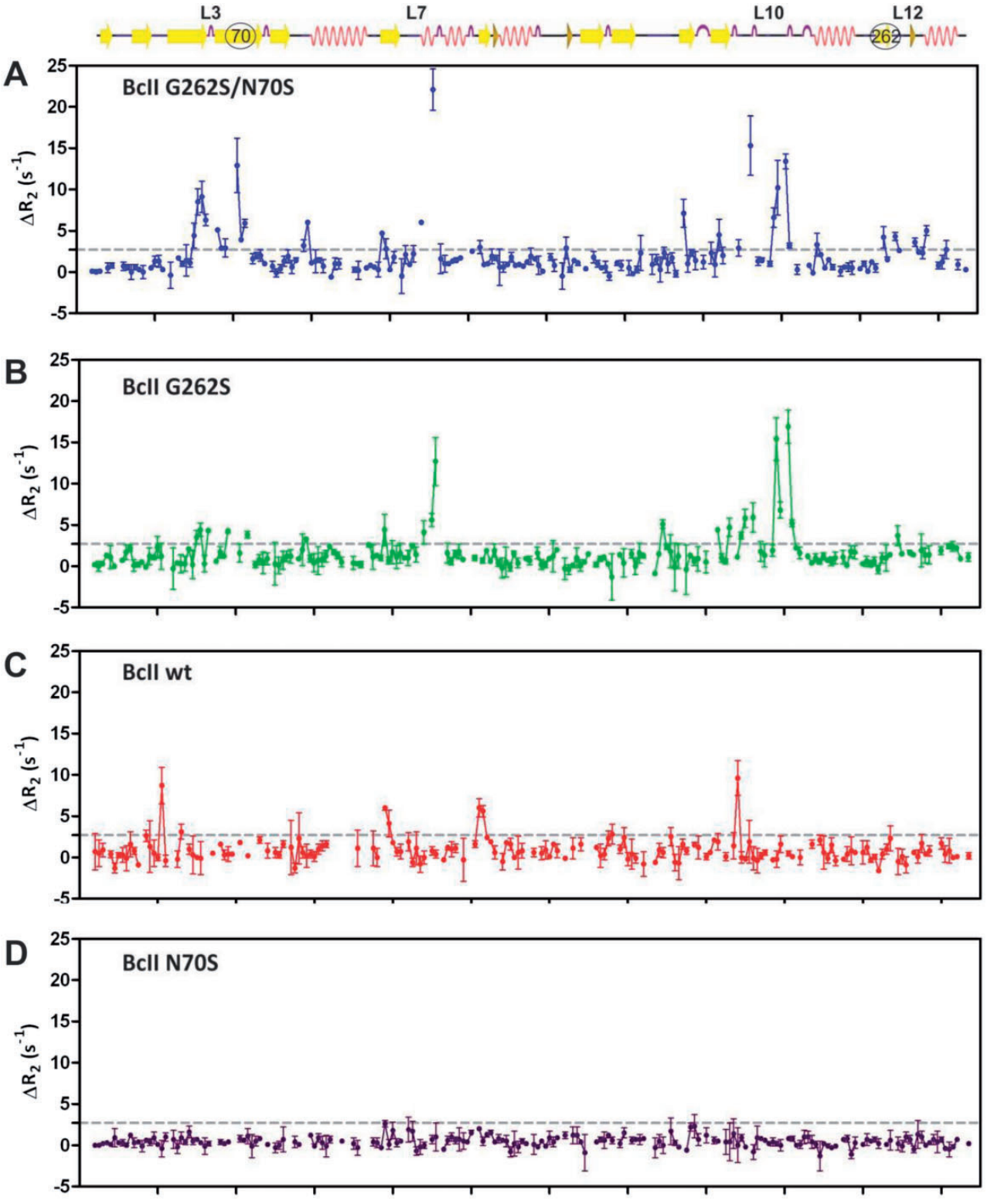

Fig. 2. ^{15}N CPMG relaxation dispersion NMR data for (*A*) BcII Gly262Ser/Asn70Ser, (*B*) BcII Gly262Ser, (*C*) wild-type BcII, and (*D*) BcII Asn70Ser as a function of residue number. The ΔR_2 values were calculated as $\Delta R_2 = R_{2,\mathrm{eff}}(\nu_{\mathrm{CPMG}} = 33) - R_{2,\mathrm{eff}}(\nu_{\mathrm{CPMG}} = 966)$, where $R_{2,\mathrm{eff}}(\nu_{\mathrm{CPMG}} = 33)$ and $R_{2,\mathrm{eff}}$ ($\nu_{\mathrm{CPMG}} = 966$) are the effective ^{15}N R_2 rates at 33 and 966 Hz CPMG frequency, respectively. Positions 70 and 262 according to BBL numbering are indicated as circles.

aim we worked with two mutations on the lactamase BcII, which have already been reported to present a strong epistatic effect on catalysis and resistance conferred to a bacterial host against β-lactams.

Gly262Ser and Asn70Ser together produce a large increase in fitness, while individually only Gly262Ser is beneficial in the wild-type background and Asn70Ser is deleterious for the enzyme activity. This epistatic effect was reported for the

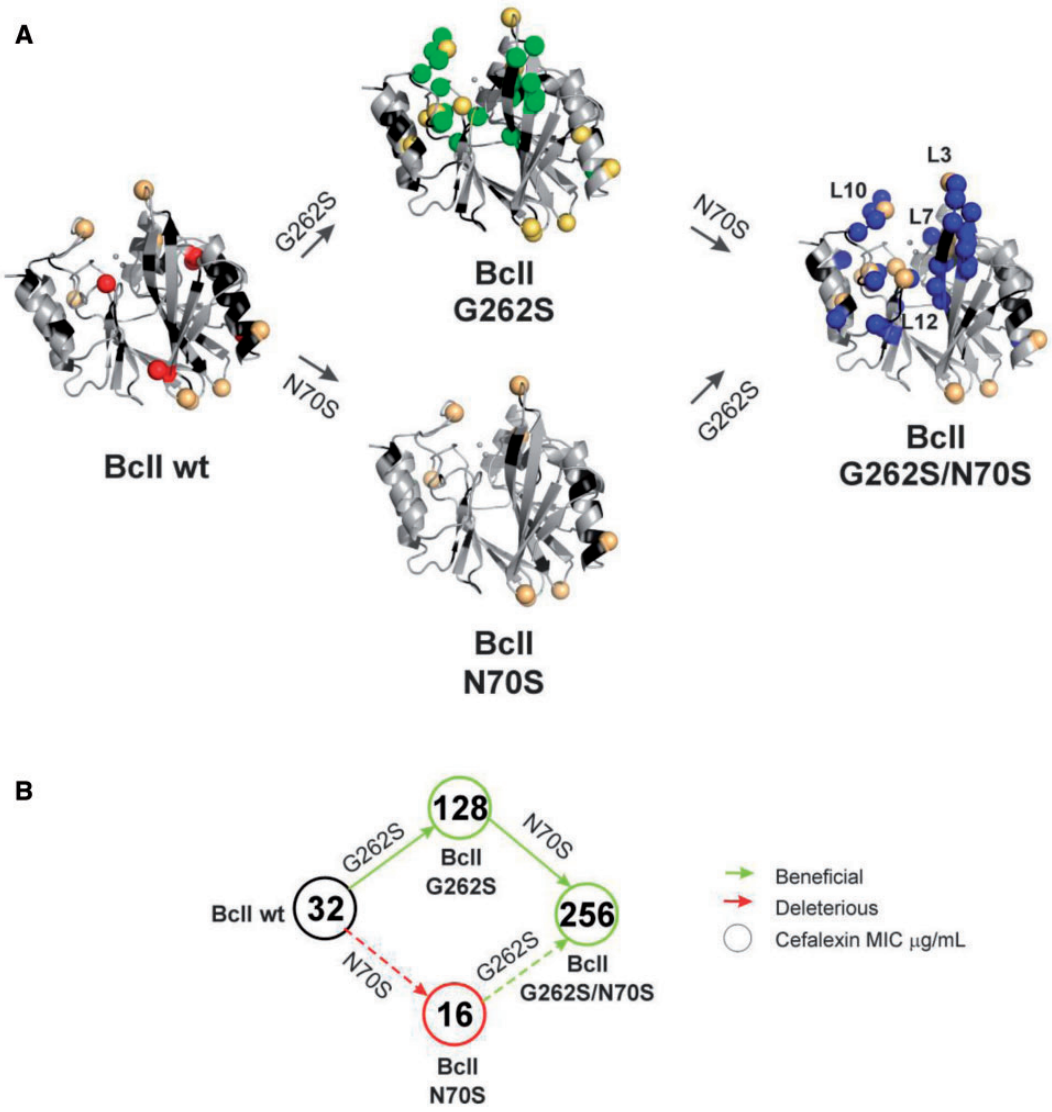

Fig. 3. (*A*) Residues with conformational exchange in the μs–ms timescale identified by ^{15}N CPMG experiments mapped onto the X-ray structure of BcII as red spheres (BcII wt), green spheres (BcII Gly262Ser), and blue spheres (BcII Gly262Ser/Asn70Ser). Residues with ms-s timescale dynamics (missing correlations in ^{1}H,^{15}N-HSQC spectra) are identified as orange spheres in all variants. Prolines and residues with overlapped resonances are colored black and residues with no exchange are colored gray. (*B*) The epistatic evolutionary trajectory followed during BcII evolution from wild-type BcII to the evolved mutant BcII Gly262Ser/Asn70Ser (Meini et al. 2015). Minimum inhibitory concentration (MIC) values taken from Meini et al. (2015) are sequentially ordered according to increasing number of mutations, from wild-type to the Gly262Ser/Asn70Ser mutant. Arrows indicate whether the mutation added is beneficial (green) or deleterious (red) in that genetic background. The circle colors indicate whether the variant shows an increment (green) or a decrease (red) in the MIC value relative to wild-type BcII. The trajectory including the deleterious mutation is represented by a dotted arrow, which is not expected to be successful under strong selection pressure, that is, the conditions that led to selection of mutant M5 (Tomatis et al. 2005).

activity of the enzyme toward cephalexin, the substrate used for the in vitro evolution experiment (Tomatis et al. 2008). Here we study the NMR spectra and dynamics of the two single mutants (Gly262Ser and Asn70Ser) and the double mutant compared with wt BcII, defining two alternative evolutionary pathways. The profile of residues undergoing fast protein dynamics (in the ps–ns timescale) is very similar among all four protein variants. However, differences arise when the slow dynamics features, those operative during substrate binding and catalysis, are probed. Our results, based on robust NMR observables sensitive to μs-ms (CPMG experiments) and slower-than-ms (exchange broadening of the resonances) motions, clearly point at several residues that undergo dynamics in these timescales to different extents: Only few residues in Asn70Ser and increasingly more in the wild-type, Gly262Ser, and Asn70Ser/Gly262Ser variants.

Within a Darwinian evolutionary perspective, a new function can be developed based on an extant or an incipient functionality (Nobeli et al. 2009; Tokuriki and Tawfik 2009). Mutation Gly262Ser acts as a switch altering substantially the slow timescale conformational dynamics in the loops that surround the active site, enabling a larger substrate spectrum. Then, mutation Asn70Ser introduced in BcII Gly262Ser confers further dynamics. These results account for the expansion

of the substrate profile in this evolutionary trajectory reported by us (Meini et al. 2015), confirming the link between conformational dynamics and expansion of substrate profile.

In contrast, mutation Asn70Ser in the wild-type background exerts an opposite effect on enzyme dynamics. This mutation quenches the dynamics observed in the wild-type BcII and hence rigidifies the structure in this timescale. In other words, mutation Asn70Ser exerts an epistatic effect on conformational dynamics. This effect parallels also the catalytic behavior of the enzyme, because the Asn70Ser mutation in BcII has a deleterious effect on catalysis and resistance. Despite these data represent a short evolutionary pathway, our study provides direct evidence on how conformational dynamics can be optimized during evolution, especially showing that epistasis can operate on this trait mirroring epistatic effects on substrate profile.

The role of protein dynamics in protein evolution has been tackled from two main viewpoints. One considers that mutations change dynamics resulting in altered or novel functions. The close correlation between changes in conformational dynamics and substrate promiscuity in our study support this notion at the atomistic level, avoiding possible structural biases in solving structures with bound ligands. The other viewpoint implies the concept that residues in flexible protein regions are more tolerant to substitutions, although this fact likely arises from a combination of dynamics, low buriedness, and low packing (Huang et al. 2014; Shahmoradi et al. 2014). This latter concept is of course entangled with the former, because areas with larger structural fluctuations can more easily rearrange to accommodate new substrates in an enzyme's active site. Our view allows us to integrate these elements to suggest how evolution manages protein flexibility. More packed regions imply more buried residues and hence less flexibility, making structural and dynamic remodeling harder to achieve through mutation. On the contrary, loose, dynamic regions like loops around active sites can on one side tolerate substitutions better than packed regions, and on the other hand be more easily restructured to achieve new functions or bind new substrates like in the case presented here. These two aspects (i.e., low impact of mutations on stability and structural and dynamic sensitivity to mutations) make loose, dynamic regions more adaptable to new functions (Abriata et al. 2012). Tokuriki and Tawfik have suggested that RNA-based viruses might evolve more rapidly because they contain many intrinsically disordered proteins, in line with this concept (Tokuriki et al. 2009). But noteworthy, our findings imply slow-timescale dynamics being created by the mutations in regions that are largely rigid in the less active enzymes (wild-type and notably Asn70Ser) but with no big changes in the structure and therefore in the packing density or buriedness, that is, implying true remodeling of the intrinsic dynamics.

On closing, we have presented an experimental description of how conformational dynamics on a catalytically relevant timescale is optimized along an epistatic evolutionary pathway. We conclude that slow conformational dynamics is an evolvable trait that can be exploited to generate new functions, of course as long as the overall protein stability is not compromised.

Materials and Methods

Protein Preparation

Wild-type BcII and the Asn70Ser, Gly262Ser, and Gly262Ser/Asn70Ser variants containing residues 27–291 (BBL numbering) were cloned into the pET28 (+) plasmid (Novagen) using NdeI and SalI restriction sites and the proteins were overexpressed in *Escherichia coli* BL21(DE3). The bacterial culture was grown at 37 °C in M9 minimal medium supplemented with ^{15}N or ^{13}C and ^{15}N (Cambridge Isotope Laboratories, Inc.) isotopes until it reached $OD_{600} = 0.6$. Protein expression was induced by addition of 0.5 mM isopropyl β-D-1-thiogalactopyranoside to the medium. At the moment of induction of protein expression, the growth medium was supplemented with 0.5 mM $ZnSO_4$ to ensure the correct folding of the overexpressed MBL. Cells were incubated overnight at 18 °C for protein expression. All subsequent purification steps were performed at 4 °C. Cells were harvested and resuspended in Buffer A (50 mM Tris–Cl pH 8.0, 200 mM NaCl), and supplemented with 10 μg/ml DNAse, 4 mM $MgCl_2$, and 2 mM phenylmethylsulfonyl fluoride. *Escherichia coli* cells were disrupted by sonication (5 cycles of 30 s with 1 min between) and the insoluble material was removed by centrifugation for 60 min at 15,000 × g. The crude extract was loaded in a Ni-sepharose resin equilibrated with Buffer A, the column was washed with 100 ml of Buffer A, and His6x-BcII was eluted with Buffer B (50 mM Tris–Cl pH 8.0, 200 mM NaCl, 500 mM imidazole) using a linear gradient (0–100% Buffer B, in 100 mL). Then, 100 μM His6x-BcII was mixed with thrombin protease (1:50 thrombin:His6x-BcII ratio) and the mixture was incubated for 3 h at 26 °C. BcII was loaded in a Ni-sepharose resin to separate it from the His6x tag and the uncleaved fusion protein, by collecting it in the flow-through. Finally, the sample was diluted (1:5) in Buffer C (100 mM 4-(2-hydroxyethyl)-1-piperazineethanesulfonic acid [HEPES] pH 7.0, 1 mM $ZnSO_4$) and loaded in a carboxymethyl (CM)-sepharose resin equilibrated with the same buffer. The column was washed with 100 ml of Buffer C and BcII was eluted with Buffer D (100 mM HEPES pH 7.0, 1 mM $ZnSO_4$, 400 mM NaCl) with a purity >95% as determined by sodium dodecyl sulfate polyacrylamide gel electrophoresis MIC: minimum inhibitory concentration (SDS-PAGE). The pure protein was concentrated using Centricon ultrafiltration devices (Millipore, Bedford, MA). The average protein yield was 10 mg/l culture. Protein concentrations were determined from the absorbance at 280 nm using a molar absorption coefficient (ε_{280}) of 30,500/M/cm.

Nuclear Magnetic Resonance Spectroscopy

NMR experiments were carried out in a 600 MHz Bruker Avance II Spectrometer equipped with a triple resonance inverse (TXI) probe head. All experiments were carried out at 298 K using standard techniques. The protein samples were analyzed at 500 μM in 100 mM MES pH 6.4, 200 mM NaCl, and 10% D_2O. Resonance assignments for wild-type BcII were

taken from the literature (Karsisiotis et al. 2013) and transferred by us to the sample conditions used in this work. ^{15}N TOCSY-HSQC experiment was used to confirm the assignment. All spectra were acquired and processed in TopSpin 2.1 (Bruker) and analyzed with Sparky 3 and CARA. Backbone resonances for BcII Asn70Ser, BcII Gly262Ser, and BcII Gly262Ser/Asn70Ser were assigned on the basis of the three-dimensional HNCO, HN(CA)CO, HN(CO)CA, HNCA, CBCA(CO)NH, and HNCACB spectra (Gardner and Kay 1998). CSPs for NH resonances were calculated according to equation (1):

$$\mathrm{CSP(ppm)} = \sqrt{\Delta\left(^{1}\mathrm{H}\right)^{2} + \frac{\Delta\left(^{15}\mathrm{N}\right)^{2}}{25}} \qquad (1)$$

Protein mobility was studied in BcII wild-type, BcII Asn70Ser, BcII Gly262Ser, and BcII Gly262Ser/Asn70Ser in a wide timescale. Fast dynamics (ps–ns) was followed by ^{15}N nuclear spin relaxation experiments as described in the literature (Lipari and Szabo 1982a, 1982b). Data analysis was performed according to the model-free formalism using Tensor v2.06 (Cordier et al. 1998). In all cases data analysis was performed using the crystal structure PDB code 4NQ4. Dynamics in the μs–ms timescale was studied through constant-time Carr–Purcell–Meiboom–Gill (CPMG) relaxation dispersion experiments (Loria et al. 1999; Millet et al. 2000) by measuring the effective transverse relaxation rate ($R_{2,\mathrm{eff}} = R_2^{\circ} + R_{ex}$) as a function of the repetition rate of 180° pulses applied during the T_2 delay, which was kept constant at 60 ms. A total of 10–12 ν_{CPMG} values, ranging from 33 to 966 Hz, and a reference spectrum were collected and the $R_{2,\mathrm{eff}}$ calculated as $\ln(I_{\mathrm{ref}}/I)/\tau_{cp}$. Dispersion profiles for residues with ΔR_2 values higher than a threshold arbitrarily defined considering the experimental noise were fitted against CPMG frequency ($1/\tau_{cp}$) to three different models implemented in the software NESSY (Bieri and Gooley 2011) (Model 1: No exchange; Model 2: Two-states, fast exchange; Model 3: Two-states, slow exchange) (supplementary figs. S4–S6 and tables S2–S4, Supplementary Material online). These fitting procedures were only carried out to determine residues which undergo dynamics; our conclusions do not depend on the parameters obtained from these fits.

Nessy Analysis

Model selection for the analysis of CPMG curves was performed by using NESSY and parameters extraction involves hypothesis testing by the calculation of the intrinsic relaxation rate $R_{2,\mathrm{intr}}$ ($R_{2,\mathrm{eff}}$ at infinite ν_{CPMG}) and $R_{2,\mathrm{eff}}$ by NESSY as described below:

$$R_{2,eff} = \frac{1}{T_{CPMG}} \times \ln\left(\frac{I_{(0)}}{I_{(\nu_{CMMG})}}\right)$$

where ν_{CPMG} is the spinlock field strength in Hz; T_{CPMG} the constant time delay in s; $I_{(0)}$ the peak intensity at 0 Hz (reference); and $I(\nu_{CPMG})$ the peak intensity at a corresponding spin lock field strength (ν_{CPMG}).

Curve fitting was performed using the method of maximum likelihood calculated by χ^2 minimization, and the uncertainties were calculated using 500 Monte Carlo simulations, that is, default NESSY settings.

If $R_{2,\mathrm{eff}}$ equals $R_{2,\mathrm{intr}}$ for every spinlock field, no exchange is assumed and the data are fitted into Model 1. For unequal parameters the data are fitted into Model 2 which assumes a two-site fast exchange. If the criteria for Model 2 are not met then the algorithm proceeds with fitting the data in to Model 3, that is, two-site slow exchange according to the Richard–Carver equation. No three-site exchange models were considered.

Supplementary Material

Supplementary tables S1–S5 and figures S1–S7 are available at *Molecular Biology and Evolution online* (http://www.mbe.oxfordjournals.org/).

Acknowledgments

This work was supported by grants from ANPCyT and the US National Institutes of Health (1R01AI100560) to A.J.V. P.E.T. and A.J.V. are CONICET staff members. M.M.G. thanks CONICET and ANPCyT for fellowships. The NMR spectrometer was supported with grants from ANPCyT.

References

Abriata LA, Palzkill T, Dal Peraro M. 2015. How structural and physicochemical determinants shape sequence constraints in a functional enzyme. *PLoS One* 10:e0118684.

Abriata LA, Salverda ML, Tomatis PE. 2012. Sequence-function-stability relationships in proteins from datasets of functionally annotated variants: the case of TEM beta-lactamases. *FEBS Lett.* 586:3330–3335.

Afriat-Jurnou L, Jackson CJ, Tawfik DS. 2012. Reconstructing a missing link in the evolution of a recently diverged phosphotriesterase by active-site loop remodeling. *Biochemistry* 51:6047–6055.

Beadle BM, Shoichet BK. 2002. Structural bases of stability-function tradeoffs in enzymes. *J Mol Biol.* 321:285–296.

Bhabha G, Lee J, Ekiert DC, Gam J, Wilson IA, Dyson HJ, Benkovic SJ, Wright PE. 2011. A dynamic knockout reveals that conformational fluctuations influence the chemical step of enzyme catalysis. *Science* 332:234–238.

Bieri M, Gooley PR. 2011. Automated NMR relaxation dispersion data analysis using NESSY. *BMC Bioinformatics* 12:421.

Boehr DD, Dyson HJ, Wright PE. 2006. An NMR perspective on enzyme dynamics. *Chem Rev.* 106:3055–3079.

Boehr DD, Nussinov R, Wright PE. 2009. The role of dynamic conformational ensembles in biomolecular recognition. *Nat Chem Biol.* 5:789–796.

Breen MS, Kemena C, Vlasov PK, Notredame C, Kondrashov FA. 2012. Epistasis as the primary factor in molecular evolution. *Nature* 490:535–538.

Cordier F, Caffrey M, Brutscher B, Cusanovich MA, Marion D, Blackledge M. 1998. Solution structure, rotational diffusion anisotropy and local backbone dynamics of *Rhodobacter capsulatus* cytochrome c2. *J Mol Biol.* 281:341–361.

Dellus-Gur E, Elias M, Caselli E, Prati F, Salverda ML, de Visser JA, Fraser JS, Tawfik DS. 2015. Negative epistasis and evolvability in TEM-1 beta-lactamase—the thin line between an enzyme's conformational freedom and disorder. *J Mol Biol.* 427:2396–2409.

DePristo MA, Weinreich DM, Hartl DL. 2005. Missense meanderings in sequence space: a biophysical view of protein evolution. *Nat Rev Genet.* 6:678–687.

Garau G, García-Sáez I, Bebrone C, Anne C, Mercuri P, Galleni M, Frère JM, Dideberg O. 2004. Update of the standard numbering scheme for class B beta-lactamases. *Antimicrob Agents Chemother*. 48:2347–2349.

Gardner KH, Kay LE. 1998. The use of 2H, 13C, 15N multidimensional NMR to study the structure and dynamics of proteins. *Annu Rev Biophys Biomol Struct*. 27:357–406.

Gong LI, Bloom JD. 2014. Epistatically interacting substitutions are enriched during adaptive protein evolution. *PLoS Genet*. 10:e1004328.

Gong LI, Suchard MA, Bloom JD. 2013. Stability-mediated epistasis constrains the evolution of an influenza protein. *Elife* 2:e00631.

Huang TT, del Valle Marcos ML, Hwang JK, Echave J. 2014. A mechanistic stress model of protein evolution accounts for site-specific evolutionary rates and their relationship with packing density and flexibility. *BMC Evol Biol*. 14:78.

Jackson CJ, Foo JL, Tokuriki N, Afriat L, Carr PD, Kim HK, Schenk G, Tawfik DS, Ollis DL. 2009. Conformational sampling, catalysis, and evolution of the bacterial phosphotriesterase. *Proc Natl Acad Sci U S A*. 106:21631–21636.

Jarymowycz VA, Stone MJ. 2006. Fast time scale dynamics of protein backbones: NMR relaxation methods, applications, and functional consequences. *Chem Rev*. 106:1624–1671.

Kaltenbach M, Tokuriki N. 2014. Dynamics and constraints of enzyme evolution. *J Exp Zool B Mol Dev Evol*. 322:468–487.

Karsisiotis AI, Damblon C, Roberts GC. 2014. Complete (1)H, (1)(5)N, and (1)(3)C resonance assignments of *Bacillus cereus* metallo-beta-lactamase and its complex with the inhibitor R-thiomandelic acid. *Biomol NMR Assign* 8:313–318.

Kay LE. 2016. New views of functionally dynamic proteins by solution NMR spectroscopy. *J Mol Biol*. 428:323–331.

Korzhnev DM, Kay LE. 2008. Probing invisible, low-populated states of protein molecules by relaxation dispersion NMR spectroscopy: an application to protein folding. *Acc Chem Res*. 41:442–451.

Liberles DA, Teichmann SA, Bahar I, Bastolla U, Bloom J, Bornberg-Bauer E, Colwell LJ, de Koning AP, Dokholyan NV, Echave J, et al. 2012. The interface of protein structure, protein biophysics, and molecular evolution. *Protein Sci*. 21:769–785.

Lindahl E. 2015. Molecular dynamics simulations. In: Kukol A, editor. *Molecular modeling of proteins*. New York: Springer p. 3–26.

Lipari G, Szabo A. 1982a. Model-free approach to the interpretation of nuclear magnetic resonance relaxation in macromolecules. 1. Theory and range of validity. *J Am Chem Soc*. 104:4546–4559.

Lipari G, Szabo A. 1982b. Model-free approach to the interpretation of nuclear magnetic resonance relaxation in macromolecules. 2. Analysis of experimental results. *J Am Chem Soc*. 104:4559–4570.

Lisi GP, Loria JP. 2016. Solution NMR spectroscopy for the study of enzyme allostery. *Chem Rev*. DOI: 10.1021/acs.chemrev.5b00541

Liu Y, Bahar I. 2012. Sequence evolution correlates with structural dynamics. *Mol Biol Evol*. 29:2253–2263.

Loria JP, Rance M, Palmer AG. 1999. A relaxation-compensated Carr—Purcell—Meiboom—Gill sequence for characterizing chemical exchange by NMR spectroscopy. *J Am Chem Soc*. 121:2331–2332.

Maurice F, Broutin I, Podglajen I, Benas P, Collatz E, Dardel F. 2008. Enzyme structural plasticity and the emergence of broad-spectrum antibiotic resistance. *EMBO Rep*. 9:344–349.

Mehta SC, Rice K, Palzkill T. 2015. Natural variants of the KPC-2 carbapenemase have evolved increased catalytic efficiency for ceftazidime hydrolysis at the cost of enzyme stability. *PLoS Pathog*. 11:e1004949.

Meini MR, Tomatis PE, Weinreich DM, Vila AJ. 2015. Quantitative description of a protein fitness landscape based on molecular features. *Mol Biol Evol*. 32:1774–1787.

Millet O, Loria JP, Kroenke CD, Pons M, Palmer AG. 2000. The static magnetic field dependence of chemical exchange linebroadening defines the NMR chemical shift time scale. *J Am Chem Soc*. 122:2867–2877.

Natarajan C, Inoguchi N, Weber RE, Fago A, Moriyama H, Storz JF. 2013. Epistasis among adaptive mutations in deer mouse hemoglobin. *Science* 340:1324–1327.

Nobeli I, Favia AD, Thornton JM. 2009. Protein promiscuity and its implications for biotechnology. *Nat Biotechnol*. 27:157–167.

Oelschlaeger P, Mayo SL, Pleiss J. 2005. Impact of remote mutations on metallo-beta-lactamase substrate specificity: implications for the evolution of antibiotic resistance. *Protein Sci* 14:765–774.

Palmer AG 3rd. 2015. Enzyme dynamics from NMR spectroscopy. *Acc Chem Res*. 48:457–465.

Perez A, Morrone JA, Simmerling C, Dill KA. 2016. Advances in free-energy-based simulations of protein folding and ligand binding. *Curr Opin Struct Biol*. 36:25–31.

Pollock DD, Thiltgen G, Goldstein RA. 2012. Amino acid coevolution induces an evolutionary Stokes shift. *Proc Natl Acad Sci U S A*. 109:E1352–E1359.

Risso VA, Manssour-Triedo F, Delgado-Delgado A, Arco R, Barroso-delJesus A, Ingles-Prieto A, Godoy-Ruiz R, Gavira JA, Gaucher EA, Ibarra-Molero B, et al. 2015. Mutational studies on resurrected ancestral proteins reveal conservation of site-specific amino acid preferences throughout evolutionary history. *Mol Biol Evol*. 32:440–455.

Salverda ML, Dellus E, Gorter FA, Debets AJ, van der Oost J, Hoekstra RF, Tawfik DS, de Visser JA. 2011. Initial mutations direct alternative pathways of protein evolution. *PLoS Genet*. 7:e1001321.

Shahmoradi A, Sydykova DK, Spielman SJ, Jackson EL, Dawson ET, Meyer AG, Wilke CO. 2014. Predicting evolutionary site variability from structure in viral proteins: buriedness, packing, flexibility, and design. *J Mol Evol*. 79:130–142.

Tokuriki N, Oldfield CJ, Uversky VN, Berezovsky IN, Tawfik DS. 2009. Do viral proteins possess unique biophysical features? *Trends Biochem Sci*. 34:53–59.

Tokuriki N, Stricher F, Serrano L, Tawfik DS. 2008. How protein stability and new functions trade off. *PLoS Comput Biol*. 4:e1000002.

Tokuriki N, Tawfik DS. 2009. Protein dynamism and evolvability. *Science* 324:203–207.

Tomatis PE, Fabiane SM, Simona F, Carloni P, Sutton BJ, Vila AJ. 2008. Adaptive protein evolution grants organismal fitness by improving catalysis and flexibility. *Proc Natl Acad Sci U S A*. 105:20605–20610.

Tomatis PE, Rasia RM, Segovia L, Vila AJ. 2005. Mimicking natural evolution in metallo-beta-lactamases through second-shell ligand mutations. *Proc Natl Acad Sci U S A*. 102:13761–13766.

Villali J, Kern D. 2010. Choreographing an enzyme's dance. *Curr Opin Chem Biol*. 14:636–643.

Wang X, Minasov G, Shoichet BK. 2002. Evolution of an antibiotic resistance enzyme constrained by stability and activity trade-offs. *J Mol Biol*. 320:85–95.

Weinreich DM, Delaney NF, Depristo MA, Hartl DL. 2006. Darwinian evolution can follow only very few mutational paths to fitter proteins. *Science* 312:111–114.

Zou T, Risso VA, Gavira JA, Sanchez-Ruiz JM, Ozkan SB. 2015. Evolution of conformational dynamics determines the conversion of a promiscuous generalist into a specialist enzyme. *Mol Biol Evol*. 32:132–143.